Porphyrins |*Hot Paper*|

π-Extended Donor–Acceptor Porphyrins and Metalloporphyrins for Antimicrobial Photodynamic Inactivation

Anzhela Galstyan,*[a] Yogesh Kumar Maurya,[b] Halina Zhylitskaya,[b] Youn Jue Bae,[c] Yi-Lin Wu,[c, e] Michael R. Wasielewski,*[c] Tadeusz Lis,[b] Ulrich Dobrindt,[d] and Marcin Stępień*[b]

Abstract: Free base, zinc and palladium π-extended porphyrins containing fused naphthalenediamide units were employed as photosensitizers in antimicrobial photodynamic therapy (aPDT). Their efficacy, assessed by photophysical and in vitro photobiological studies on Gram-positive bacteria, was found to depend on metal coordination, showing a dramatic enhancement of photosensitizing activity for the palladium complex.

Introduction

Multidrug resistance is a major reason for failure in the treatment of infections and thus antimicrobial strategies that do not contribute to the selection of pathogenic bacteria are currently gaining attraction.[1] In particular, antimicrobial photodynamic therapy (aPDT) has been proposed as an alternative approach for the treatment of bacterial infections.[2] In aPDT, reactive oxygen species (ROS) produced by an irradiated photosensitizer (PS) attack proteins, nucleic acids and lipids, causing bacterial cell death.[3] These ROS are generated either through electron or hydrogen transfer to substrates (type I mechanism) or by energy transfer to molecular oxygen with generation of singlet oxygen ($^1O_2$, type II mechanism).[3c–e]

Currently, porphyrin derivatives and their precursors are the most widely used PSs in clinics.[4] These include HpD (Photofrin®), Verteporfin (Visudyne®), *meso*-tetra(*m*-hydroxyphenyl)-chlorin (Foscan®), lutetium texaphyrin (Antrin®), mono-L-aspartyl chlorin e_6 (LS11), 2-(1-hexyloxyethyl)-2-divinyl pyropheophorbide *a* (Photochlor), and 1,5-aminolevulinic acid and its derivatives as precursors of protoporphyrin IX (Levulan®, Metvix®).[5] Tetrapyrrole photosensitizers mostly exhibit type II activity, but their mode of action can be tuned by varying the substituents or the central metal atom.[6] Despite widespread clinical use, porphyrin-based systems have several drawbacks, in particular their relatively low absorptivity in the visible and near-infrared regions. Since longer absorption wavelengths are strongly preferred for in vivo applications, the porphyrin ring system has been variously modified to enhance absorption in the red and near-infrared regions. This effect can be achieved through partial β-hydrogenation, as in chlorins (λ_{abs}^{max} = 650 nm) and bacteriochlorins (λ_{abs}^{max} = 780 nm).[7] However, these derivatives are generally unstable and are readily oxidized back to the corresponding porphyrins upon irradiation. Alternatively, long-wavelength absorption can be enhanced by annulation of carbo- and heterocycles to the periphery of the porphyrin.[8] However, because of the more challenging synthesis and usually low solubility of the final products in aqueous media, the use of such π-extended porphyrins used in PDT remains limited.[9]

Here we report on the use of π-extended porphyrins and metalloporphyrins as aPDT photosensitizers. The systems used in this study, labelled M-**NDP** (Scheme 1), contain four naphthalenediamide units fused to the β-pyrrolic positions of the porphyrin ring. We show that their activities against Gram-positive *Staphylococcus aureus* (*S. aureus*) 3150/12 and *Bacillus subtilis* (*B. subtilis)* DB104 are highly dependent on the metal coordination status of the porphyrin macrocycle (M = 2H, Zn and Pd).

[a] *Dr. A. Galstyan*
Center for Soft Nanoscience
Westfälische Wilhelms-Universität Münster
Busso-Peus-Straße 10, 48149 Münster (Germany)
E-mail: anzhela.galstyan@wwu.de

[b] *Dr. Y. K. Maurya, Dr. H. Zhylitskaya, Prof. Dr. T. Lis, Prof. Dr. M. Stępień*
Wydział Chemii, Uniwersytet Wrocławski
ul. F. Joliot-Curie 14, 50383 Wrocław (Poland)
E-mail: marcin.stepien@chem.uni.wroc.pl

[c] *Y. J. Bae, Dr. Y.-L. Wu, Prof. Dr. M. R. Wasielewski*
Department of Chemistry and
Institute for Sustainability and Energy at Northwestern
Northwestern University
Evanston, Illinois, 60208-3113 (USA)
E-mail: m-wasielewski@northwestern.edu

[d] *Prof. Dr. U. Dobrindt*
Institute of Hygiene
Westfälische Wilhelms-Universität Münster
Mendelstraße 7, 48149 Münster (Germany)

[e] *Dr. Y.-L. Wu*
Current address: School of Chemistry, Cardiff University
Main Building, Park Place, Cardiff CF10 3AT (UK)

Supporting information and the ORCID identification number(s) for the author(s) of this article can be found under: https://doi.org/10.1002/chem.201905372.

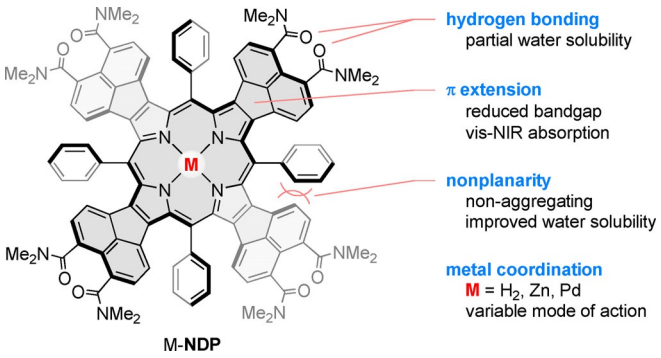

Scheme 1. Design principle of π-extended porphyrins used in this study.

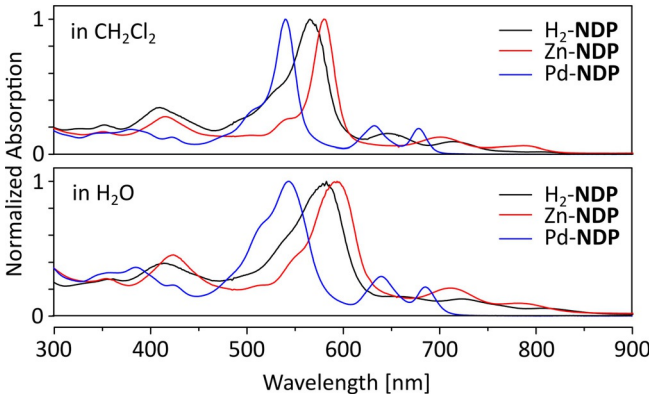

Figure 2. Optical absorbance of H_2-**NDP** (black), Zn-**NDP** (red) and Pd-**NDP** (blue) in DCM (top) and H_2O (bottom). Molar concentrations were 1×10^{-5} M.

Results and Discussion

H_2-**NDP**, obtained according to a recently reported procedure,[10] was transformed into its Zn and Pd complexes using established methods (see Supporting Information). The steric congestion around the porphyrin core in M-**NDP**, caused by combined *meso*-substitution and β-fusion, results in a significant out-of-plane distortion of the aromatic surface, clearly seen in the solid-state geometry of Pd-**NDP** (Figure 1). The dimethylaminocarbonyl substituents are twisted relative to the peripheral naphthalene units, producing additional steric bulk that precludes direct π–π-stacking interactions between molecules. As a consequence, H_2-**NDP** and Pd-**NDP** do not aggregate significantly in organic solvents, as evidenced by their concentration-independent optical absorption spectra. Zn-**NDP** was previously found to undergo specific aggregation in chloroform solutions,[10] which was attributed to intermolecular coordination of amide substituents to Zn centres in Zn-**NDP**. The latter effect was however observed at relatively high concentrations (ca. 10^{-2} to 10^{-3} M) and it appears to have no significant influence on the absorption spectra of Zn-NDP recorded for more dilute samples (10^{-5} to 10^{-6} M, Figure S5, Supporting Information). While DLS data obtained in water (Figure S9, Supporting Information) indicate the formation of nanoparticles, absorption spectra of **NDP**s remain concentration-independent in the 10^{-5} to 10^{-6} M range (Figure S6), and resemble those observed in DCM solutions.

Photophysical properties were initially measured in dichloromethane (DCM) to assess the PS performance (Figure 2 and Table 1). All **NDP** photosensitizers showed absorption bands extending from 300 to 700 nm, presenting multiple opportunities for electronic excitation in close proximity to the near-infrared spectral range. The most intense absorption maxima of the M-**NDP** dyes appear at 541–573 nm and are bathochromically shifted relative to the Soret bands of hematoporphyrin (395 nm) and protoporphyrin IX (398 nm) in DCM, consistent with the expanded π-conjugation of the **NDP** chromophore. Molar extinction coefficients of the largest peaks (> 10^5 L mol^{-1} cm^{-1}, Table S2, in the Supporting Information) are comparable for all derivatives and consistent with the previous report. As observed previously for other palladium(II) porphyrins, the Soret and Q bands of Pd-**NDP** are blueshifted in comparison with Zn-**NDP** and H_2-**NDP**, with a characteristic intensity increase of the Q(1,0) transition.[11] This observed trend is semi-quantitatively reproduced by time-dependent density functional theory (TD-DFT) calculations which reveal a larger optical band gap in the Pd-NDP system relative to the Zn-**NDP** and H_2-**NDP** chromophores (see Supporting Information), in line with the experiment. This change is mostly attributed to the lower energy of the HOMO level in the Pd-**NDP** complex.

Importantly for their prospective application as PSs, each of the three M-**NDP** derivatives could be solubilized in water

Table 1. Photophysical data for H_2-**NDP**, Zn-**NDP**, and Pd-**NDP**.

PS	log$P_{o/w}$[a]	Φ_Δ[b] (DCM)	Φ_Δ[b] (H_2O)	Triplet states[c]		
				λ_{ex} [nm]	$\tau_{S\rightarrow T}$[d] [ps]	$\tau_{T\rightarrow GS}$[e] [μs]
H_2-**NDP**	0.31	0.59	0.50	600	605 ± 2	54 ± 1 210 ± 10
Zn-**NDP**	0.32	0.57	0.07	580	530 ± 10	77 ± 1 250 ± 10
Pd-**NDP**	0.51	1.00	0.39	540	2.6 ± 0.1	20 ± 1 52 ± 3

[a] 1-Octanol/water partition coefficient. [b] Quantum yields of singlet oxygen photogeneration measured using the relative method and methylene blue as a reference. Estimated accuracy ±0.03. [c] Triplet formation and decay (deoxygenated dichloromethane, excitation at λ_{ex}). [d] Singlet (S) to triplet (T) intersystem crossing. [e] Decay of triplet (T) to the ground state (GS); the observed biexponential decay may be related to (i) collisional triplet-triplet annihilation and/or (ii) aggregation/conformation changes (see the Supporting Information for additional discussion).

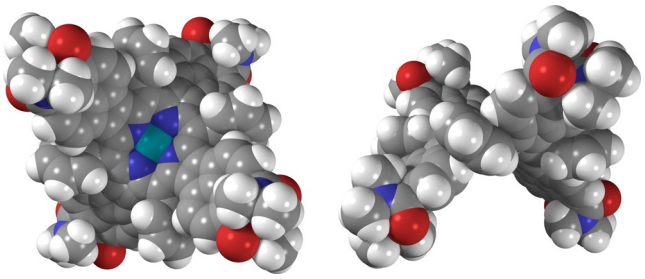

Figure 1. Molecular geometry of Pd-**NDP**, obtained from an X-ray crystallographic analysis, showing the deep saddle distortion of the chromophore.

(containing less than 1% DMSO), at practically useful concentrations (ca. 10^{-5} M). This solubility enhancement, which is also reflected in the log$P_{o/w}$ values (Table 1), is caused by the combination of amide substitution and non-planarity of the **NDP** chromophore. Pd-**NDP** is the least soluble in water among the three derivatives. In aqueous media, absorption bands of the M-**NDP** systems are broadened and redshifted. This effect is more pronounced for H_2-**NDP** and Zn-**NDP** (17 and 18 nm, respectively, for the Soret band) and is apparently consistent with the positive solvatochromism observed for related donor–acceptor oligopyrroles.[12] The absorptivity of Pd-**NDP** in water is significantly lower than measured for H_2-**NDP** and Zn-**NDP**, possibly indicating a more aggregated state of Pd-**NDP** in this solvent. All M-**NDP** derivatives display negligible fluorescence in solution ($\Phi_{fl} \ll 1\%$), suggesting an excited-state decay pathway competitive to singlet emission, caused by the non-planar structures of these π-extended chromophores (see below).

Excited-state lifetimes of the three PSs were measured in deoxygenated dichloromethane using transient absorption spectroscopy (Table 1 and Supporting Information). As suggested by the μs lifetimes, all three **NDP** derivatives form triplets, likely through the spin-orbit coupling mechanism. In the case of Pd-**NDP**, the heavy-metal effect enhances intersystem crossing as shown in the shorter triplet formation time constant, $\tau_{S\rightarrow T}$. In addition, $\tau_{S\rightarrow T}$ for H_2-**NDP** and Zn-**NDP** (605 ± 2 and 530 ± 10 ps, respectively), are reduced relative to the value determined for zinc(II) *meso*-tetraphenylporphyrin (Zn**TPP**, ≈2000 ps in toluene),[13] and compare well with the time constant reported for zinc(II) *meso*-tetraphenyltetrabenzoporphyrin (ZnTBTPP, 291 ± 7 ps in toluene).[14] In the case of ZnTBTPP and M-**NDP**s, the saddle distortion of the chromophore may be a major source of spin-orbit coupling.[15] This rapid triplet formation accounts for the observed low fluorescence and suggests applicability of **NDP** dyes for oxygen sensitization.

Irreversible photooxidation of 1,3-diphenylisobenzofuran (DPBF), a non-selective probe for singlet oxygen and reactive oxygen species, was used to evaluate the ability of the M-**NDP** dyes to generate ROS in DCM. In these experiments, methylene blue (MB), was used as the reference (Figure 3). Upon irradiation with visible light (xenon lamp, 5 mW cm^{-2}, $\lambda > 515$ nm), all M-**NDP** porphyrins produced significant decay of the DPBF absorption, monitored at 414 nm. The quantum yield of singlet oxygen photogeneration of Pd-**NDP** in DCM (Table 1) was

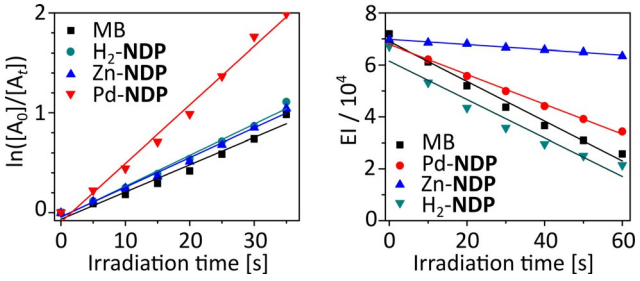

Figure 3. (a) The plot of DPBF absorbance change and (b) ABMDMA emission change as a function of irradiation time. DPBF, 1,3-diphenylisobenzofuran; ABMDMA, 9,10-anthracenediyl-bis(methylene) dimalonic acid; EI, emission intensity integral.

higher than the values determined for Zn-**NDP** and H_2-**NDP**, reflecting the heavy atom effect of Pd, which increases the yield of intersystem crossing from the excited singlet to lowest energy triplet excited state. A quantitative analysis of photooxidation reactions leading to the loss of emission (409 and 431 nm) of the water-soluble anthracene 9,10-dipropionic acid (ABMDMA) was used to measure $^1O_2$ production in aqueous media. In contrast to the measurements in DCM, Pd-**NDP** and H_2-**NDP** exhibit greater singlet oxygen quantum yields in comparison with Zn-**NDP**.

Since the M-**NDP** photosensitizers are not positively charged, they are most suitable to target Gram-positive bacteria.[16] We choose two representative strains, *S. aureus* 3150/12 and *B. subtilis* DB104, to study antibacterial activity of M-**NDP**s. Pathogens such as *S. aureus* are one of the major causes of community and hospital-acquired infections, with significant morbidity and mortality. The non-pathogenic *B. subtilis* is a normal gut commensal in humans and is considered the best studied Gram-positive bacterium. Killing assays were performed after incubation of ca. 10^8 colony-forming unit mL^{-1} (CFU mL^{-1}) with 10 μM of the corresponding M-**NDP** for 15 min and plating aliquots after a certain time of irradiation (30, 60 and 90 min) with light passing through a 515 nm cut-off filter. The results of the determination of antibacterial effect are summarized in Figure 4.

Under identical conditions, the viability of both strains showed significant dependence on the porphyrin derivative used. Pd-**NDP** was found to be more potent against both tested bacteria with different inactivation kinetics. For instance, no colony was found on the agar plate when *S. aureus* 3150/12 was treated with Pd-**NDP** and irradiated for 60 min (18 J cm^{-2}). This was not the case when *B. subtilis* DB104 was used. Nevertheless bactericidal effect (>3 log$_{10}$ steps reduction) and disinfecting effect (>5 log$_{10}$ steps reduction) could be achieved after 60 min and 90 min irradiation, correspondingly. H_2-**NDP** and Zn-**NDP** showed to be less active with both bacterial strains. However, when treated with H_2-**NDP** and light (90 min, 27 J cm^{-2}), the reduction in log$_{10}$ unit was 3.15 for *S. aureus* 3150/12 and 4.47 for *B. Subtilis* DB104, respectively. Under identical irradiation conditions Zn-**NDP** effected a reduction of less than 3 log$_{10}$ units. Visual inspection of the fluorescence images of Live/Dead stained *S. aureus* 3150/12 after incubation with M-**NDP**s and irradiation with 9 J cm^{-2} light doses further confirmed the activity of Pd-**NDP** (Figure S18, Supporting Information). Numerous viable microorganisms (green fluorescence) were visible in the control sample and in the samples of *S. aureus* 3150/12 treated with H_2-**NDP** and Zn-**NDP**. In contrast, a large number of dead bacterial cells (red fluorescence) appeared when Pd-**NDP** was used. The fluorescence images of *B. subtilis* DB104 treated with M-**NDP** and irradiated under similar conditions showed mostly viable bacteria, consistent with the results of CFU counting.

The markedly lower photocytotoxicities of H_2-**NDP** and Zn-**NDP** compared to Pd-**NDP** suggest that important intracellular targets are damaged more efficiently when Pd-**NDP** was used. Commonly, molecular characteristics such as the targeting unit, charge, asymmetry and lipophilicity govern binding and

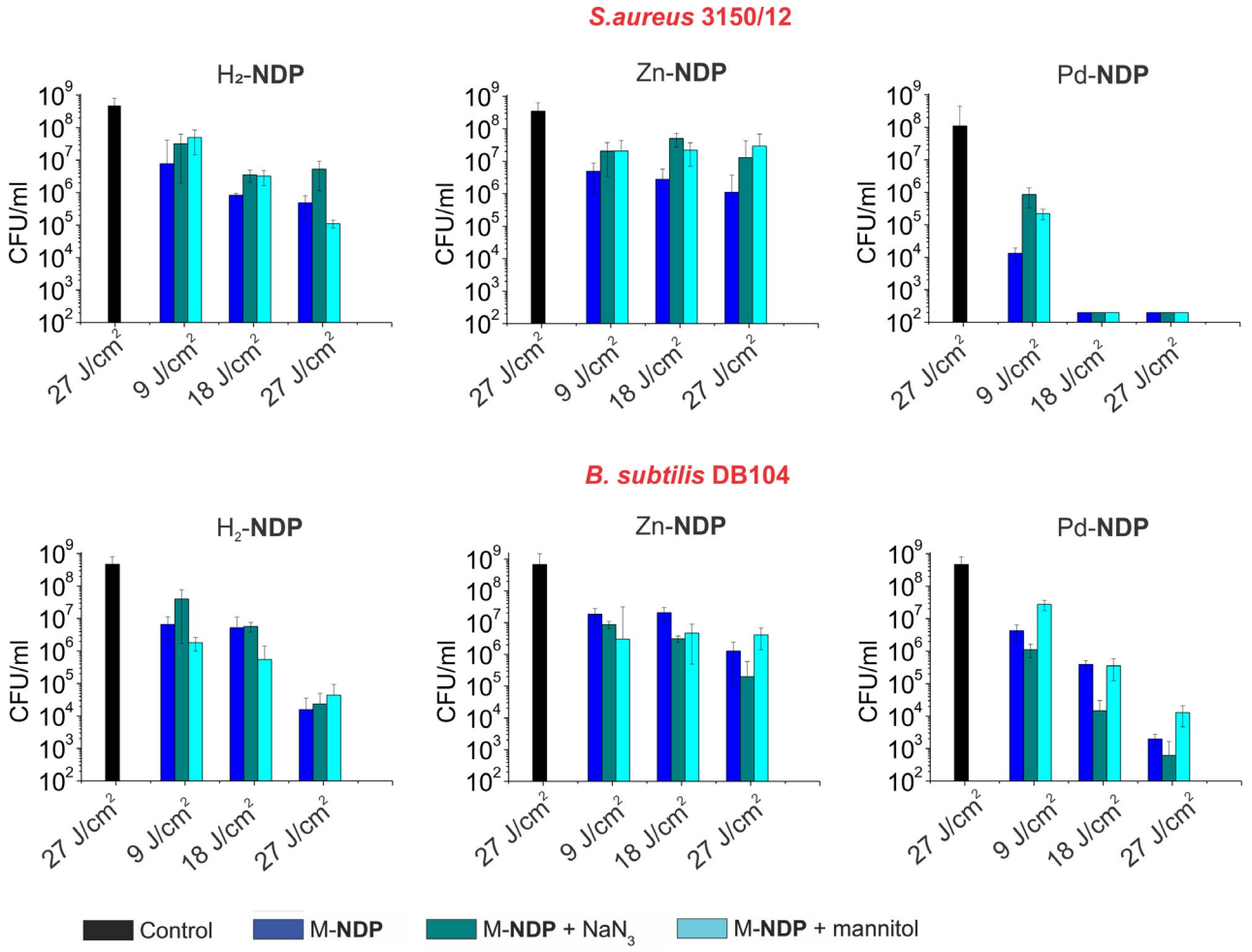

Figure 4. Histograms showing the photodynamic inactivation of *S. aureus* 3150/12 and *B. Subtilis* DB104 in planktonic cultures treated with H_2-**NDP**, Zn-**NDP**, and Pd-**NDP**. Control group are bacteria without any treatment. Irradiation conditions: $\lambda > 515$ nm, 5 Wcm^{-2}, 30, 60 and 90 min. The concentration of PSs is 10 μM.

uptake of the PS into bacterial cells.[17] Although we used a homologous set of porphyrins, Pd-**NDP** has a higher log $P_{o/w}$ value, which could contribute to improved cellular uptake and efficient damage of the bacterial cell. ROS quantum yields determined in aqueous media do not appear to be sufficient to explain the observed differences in phototoxicity. Literature reports describe that the palladium bacteriochlorin sensitizer TOOKAD can produce different reactive oxygen species in different environments.[18] Thus, to investigate the underlying mechanism of the bacterial inactivation and find out whether aPDT efficacy is affected by the nature and persistence of the ROS two different quenchers, sodium azide and mannitol, were used in irradiation experiments.[19]

Although neither of these two scavengers could provide complete protection from inactivation, both sodium azide and mannitol had an effect on the viability of microorganisms. Comparison of the photodynamic effect of Pd-**NDP** for *S. aureus* 3150/12 and *B. subtilis* DB104 in the presence of sodium azide showed that the mode of action of Pd-**NDP** is most likely different for these two strains. Whereas for *S. aureus* 3150/12 photocytotoxicity was reduced indicating that killing of bacteria was mainly due to the generation of $^1O_2$ via a type II mechanism, for *B. subtilis* DB104 potentiation of the aPDT effect was observed. Mannitol, which is known to quench hydroxyl radicals formed in the type I mechanism, was found to reduce the activity of Pd-**NDP** against both bacterial strains. These results suggest that the photosensitization by Pd-**NDP** is based on a combination of type I and type II mechanisms. For H_2-**NDP** and Zn-**NDP** this effect was not pronounced. A strain-dependent photochemical mechanism was previously reported by Hamblin et al. for a homologous series of phenothiazinium dyes.[20] The mechanism of action was proposed to depend on the microenvironment, for example, higher binding of the dye to bacteria. In another study based of series of *meso*-tetraarylporphyrins, Almeida et al. showed for the series of PSs that the mechanism of action of the certain PS depends on structure (number and placement of charges), aggregation behaviour, and affinity for the cell membrane.[21]

Conclusions

In summary, π-extended porphyrins containing peripheral naphthalenediamide subunits are examined here as aPDT photosensitizers for the first time. These systems feature intense

vis-NIR absorption, sufficient solubility in water, achieved without additional functionalization, and appreciable quantum yields of singlet oxygen photogeneration. The aPDT efficiency of M-**NDP** photosensitizers can be tuned by metal coordination, showing that this family of dyes could be used for treatment of infections caused by Gram-positive bacteria. The photosensitizing potential of other donor–acceptor oligopyrrole chromophores is currently explored in our laboratories.

Experimental Section

For full details, please see the Supporting Information.

Acknowledgements

This work was supported by the Foundation for Polish Science (TEAM POIR.04.04.00-00-5BF1/17-00, to M.S.), U.S. Department of Energy, Office of Science, Office of Basic Energy Sciences under Award DE-FG02-99ER14999 (M.R.W.), German Research Foundation (DFG GA 2362/2-1, to A.G.), and Fonds der Chemischen Industrie (to A.G.).

Conflict of interest

The authors declare no conflict of interest.

Keywords: antimicrobial · photosensitizers · singlet oxygen · triplet state · π-extended porphyrins

[1] a) A. Gupta, R. F. Landis, C.-H. Li, M. Schnurr, R. Das, Y.-W. Lee, M. Yazdani, Y. Liu, A. Kozlova, V. M. Rotello, *J. Am. Chem. Soc.* **2018**, *140*, 12137 – 12143; b) P. R. Judzewitsch, T.-K. Nguyen, S. Shanmugam, E. H. H. Wong, C. Boyer, *Angew. Chem. Int. Ed.* **2018**, *57*, 4559 – 4564; *Angew. Chem.* **2018**, *130*, 4649 – 4654; c) J. D. Steckbeck, B. Deslouches, R. C. Montelaro, *Expert Opin. Biol. Ther.* **2014**, *14*, 11 – 14; d) C. D. Fjell, J. A. Hiss, R. E. W. Hancock, G. Schneider, *Nat. Rev. Drug Discovery* **2012**, *11*, 37 – 51.

[2] a) A. Regiel-Futyra, J. M. Dąbrowski, O. Mazuryk, K. Śpiewak, A. Kyzioł, B. Pucelik, M. Brindell, G. Stochel, *Coord. Chem. Rev.* **2017**, *351*, 76 – 117; b) Y. Liu, R. Qin, S. A. J. Zaat, E. Breukink, M. Heger, *J. Clin. Transl. Res.* **2015**, *1*, 140 – 167; c) A. Galstyan, R. Schiller, U. Dobrindt, *Angew. Chem. Int. Ed.* **2017**, *56*, 10362 – 10366; *Angew. Chem.* **2017**, *129*, 10498 – 10502; d) A. Galstyan, D. Block, S. Niemann, M. C. Grüner, S. Abbruzzetti, M. Oneto, C. G. Daniliuc, S. Hermann, C. Viappiani, M. Schäfers, B. Löffler, C. A. Strassert, A. Faust, *Chem. Eur. J.* **2016**, *22*, 5243 – 5252; e) M. Wainwright, T. Maisch, S. Nonell, K. Plaetzer, A. Almeida, G. P. Tegos, M. R. Hamblin, *Lancet Infect. Dis.* **2017**, *17*, e49 – e55.

[3] a) L. M. Mink, M. L. Neitzel, L. M. Bellomy, R. E. Falvo, R. K. Boggess, B. T. Trainum, P. Yeaman, *Polyhedron* **1997**, *16*, 2809 – 2817; b) O. E. Akilov, K. O'Riordan, S. Kosaka, T. Hasan, *Med. Laser Appl.* **2006**, *21*, 251 – 260; c) H. Horiuchi, A. Sakai, S. Akiyama, R. Ikeda, S. Ito, M. Furuya, Y. Gomibuchi, M. Ichikawa, T. Yoshihara, S. Tobita, T. Okutsu, *J. Photochem. Photobiol. A* **2017**, *339*, 19 – 24; d) J.-Y. Zeng, M.-Z. Zou, M. Zhang, X.-S. Wang, X. Zeng, H. Cong, X.-Z. Zhang, *ACS Nano* **2018**, *12*, 4630 – 4640; e) S. Callaghan, M. O. Senge, *Photochem. Photobiol. Sci.* **2018**, *17*, 1490 – 1514.

[4] a) E. S. Nyman, P. H. Hynninen, *J. Photochem. Photobiol. B* **2004**, *73*, 1 – 28; b) E. Paszko, C. Ehrhardt, M. O. Senge, D. P. Kelleher, J. V. Reynolds, *Photodiagn. Photodyn. Ther.* **2011**, *8*, 14 – 29; c) V. Almeida-Marrero, E. van de Winckel, E. Anaya-Plaza, T. Torres, A. de la Escosura, *Chem. Soc. Rev.* **2018**, *47*, 7369 – 7400.

[5] a) S. Pushpan, S. Venkatraman, V. Anand, J. Sankar, D. Parmeswaran, S. Ganesan, T. Chandrashekar, *Curr. Med. Chem.: Anti-Cancer Agents* **2002**, *2*, 187 – 207; b) J. Kou, D. Dou, L. Yang, *Oncotarget* **2017**, *8*, 81591 – 81603.

[6] a) P. Mroz, J. Bhaumik, D. K. Dogutan, Z. Aly, Z. Kamal, L. Khalid, H. L. Kee, D. F. Bocian, D. Holten, J. S. Lindsey, M. R. Hamblin, *Cancer Lett.* **2009**, *282*, 63 – 76; b) H. L. Kee, J. Bhaumik, J. R. Diers, P. Mroz, M. R. Hamblin, D. F. Bocian, J. S. Lindsey, D. Holten, *J. Photochem. Photobiol. A* **2008**, *200*, 346 – 355.

[7] a) S. Schastak, S. Ziganshyna, B. Gitter, P. Wiedemann, T. Claudepierre, *PLoS ONE* **2010**, *5*, e11674; b) L. Huang, Y.-Y. Huang, P. Mroz, G. P. Tegos, T. Zhiyentayev, S. K. Sharma, Z. Lu, T. Balasubramanian, M. Krayer, C. Ruzie, E. Yang, H. L. Kee, C. Kirmaier, J. R. Diers, D. F. Bocian, D. Holten, J. S. Lindsey, M. R. Hamblin, *Antimicrob. Agents Chemother.* **2010**, *54*, 3834 – 3841.

[8] a) A. Tsuda, *Science* **2001**, *293*, 79 – 82; b) T. Tanaka, A. Osuka, *Chem. Soc. Rev.* **2015**, *44*, 943 – 969; c) J. Mack, Y. Asano, N. Kobayashi, M. J. Stillman, *J. Am. Chem. Soc.* **2005**, *127*, 17697 – 17711; d) J. Mack, *Chem. Rev.* **2017**, *117*, 3444 – 3478; e) Y. Saegusa, T. Ishizuka, K. Komamura, S. Shimizu, H. Kotani, N. Kobayashi, T. Kojima, *Phys. Chem. Chem. Phys.* **2015**, *17*, 15001 – 15011; f) H.-J. Xu, J. Mack, D. Wu, Z.-L. Xue, A. B. Descalzo, K. Rurack, N. Kobayashi, Z. Shen, *Chem. Eur. J.* **2012**, *18*, 16844 – 16867; g) C. Preihs, J. F. Arambula, D. Magda, H. Jeong, D. Yoo, J. Cheon, Z. H. Siddik, J. L. Sessler, *Inorg. Chem.* **2013**, *52*, 12184 – 12192.

[9] a) J. R. Sommer, A. H. Shelton, A. Parthasarathy, I. Ghiviriga, J. R. Reynolds, K. S. Schanze, *Chem. Mater.* **2011**, *23*, 5296 – 5304; b) C. M. B. Carvalho, T. J. Brocksom, K. T. de Oliveira, *Chem. Soc. Rev.* **2013**, *42*, 3302.

[10] H. Zhylitskaya, J. Cybińska, P. Chmielewski, T. Lis, M. Stępień, *J. Am. Chem. Soc.* **2016**, *138*, 11390 – 11398.

[11] P. J. Spellane, M. Gouterman, A. Antipas, S. Kim, Y. C. Liu, *Inorg. Chem.* **1980**, *19*, 386 – 391.

[12] a) M. Żyła-Karwowska, H. Zhylitskaya, J. Cybińska, T. Lis, P. J. Chmielewski, M. Stępień, *Angew. Chem. Int. Ed.* **2016**, *55*, 14658 – 14662; *Angew. Chem.* **2016**, *128*, 14878 – 14882; b) M. Żyła-Karwowska, L. Moshniaha, Y. Hong, H. Zhylitskaya, J. Cybińska, P. J. Chmielewski, T. Lis, D. Kim, M. Stępień, *Chem. Eur. J.* **2018**, *24*, 7525 – 7530; c) M. Navakouski, H. Zhylitskaya, P. J. Chmielewski, T. Lis, J. Cybińska, M. Stępień, *Angew. Chem. Int. Ed.* **2019**, *58*, 4929 – 4933; *Angew. Chem.* **2019**, *131*, 4983 – 4987.

[13] N. Banerji, S. V. Bhosale, I. Petkova, S. J. Langford, E. Vauthey, *Phys. Chem. Chem. Phys.* **2011**, *13*, 1019 – 1029.

[14] V. V. Roznyatovskiy, R. Carmieli, S. M. Dyar, K. E. Brown, M. R. Wasielewski, *Angew. Chem. Int. Ed.* **2014**, *53*, 3457 – 3461; *Angew. Chem.* **2014**, *126*, 3525 – 3529.

[15] G. G. Gurzadyan, T.-H. Tran-Thi, T. Gustavsson, *J. Chem. Phys.* **1998**, *108*, 385 – 388.

[16] a) G. Jori, C. Fabris, M. Soncin, S. Ferro, O. Coppellotti, D. Dei, L. Fantetti, G. Chiti, G. Roncucci, *Lasers Surg. Med.* **2006**, *38*, 468 – 481; b) Z. Malik, J. Hanania, Y. Nitzan, *J. Photochem. Photobiol. B* **1990**, *5*, 281 – 293; c) M. R. Hamblin, *J. Antimicrob. Chemother.* **2002**, *49*, 941 – 951; d) M. A. Pereira, M. A. F. Faustino, J. P. C. Tomé, M. G. P. M. S. Neves, A. C. Tomé, J. A. S. Cavaleiro, Â. Cunha, A. Almeida, *Photochem. Photobiol. Sci.* **2014**, *13*, 680.

[17] a) A. Galstyan, J. Putze, U. Dobrindt, *Chem. Eur. J.* **2018**, *24*, 1178 – 1186; b) A. Galstyan, U. Dobrindt, *J. Mater. Chem. B* **2018**, *6*, 4630 – 4637; c) C. Zhou, G. W. N. Chia, J. C. S. Ho, T. Seviour, T. Sailov, B. Liedberg, S. Kjelleberg, J. Hinks, G. C. Bazan, *Angew. Chem. Int. Ed.* **2018**, *57*, 8069 – 8072; *Angew. Chem.* **2018**, *130*, 8201 – 8204.

[18] Y. Vakrat-Haglili, L. Weiner, V. Brumfeld, A. Brandis, Y. Salomon, B. McIlroy, B. C. Wilson, A. Pawlak, M. Rozanowska, T. Sarna, A. Scherz, *J. Am. Chem. Soc.* **2005**, *127*, 6487 – 6497.

[19] A. Tavares, S. R. S. Dias, C. M. B. Carvalho, M. A. F. Faustino, J. P. C. Tomé, M. G. P. M. S. Neves, A. C. Tomé, J. A. S. Cavaleiro, Â. Cunha, N. C. M. Gomes, E. Alves, A. Almeida, *Photochem. Photobiol. Sci.* **2011**, *10*, 1659 – 1669.

[20] K. R. Kasimova, M. Sadasivam, G. Landi, T. Sarna, M. R. Hamblin, *Photochem. Photobiol. Sci.* **2014**, *13*, 1541 – 1548.

[21] C. Vieira, A. T. P. C. Gomes, M. Q. Mesquita, N. M. M. Moura, M. G. P. M. S. Neves, M. A. F. Faustino, A. Almeida, *Front. Microbiol.* **2018**, *9*, 2665.

Manuscript received: November 27, 2019
Accepted manuscript online: January 22, 2020
Version of record online: June 8, 2020

